University of Wollongong
Research Online

Faculty of Engineering - Papers (Archive)

Faculty of Engineering and Information Sciences

2011

Effect of initial static shear stress on the undrained cyclic behavior of saturated sand by torsional shear loading

Gabriele Chiaro
University of Wollongong, gchiaro@uow.edu.au

Takeshi Sato
Integrated Geotechnology Institute Ltd., tsato@iis.u-tokyo.ac.jp

Takashi Kiyota
IIS, University of Tokyo, kiyota@iis.u-tokyo.ac.jp

Junichi Koseki
IIS, University of Tokyo, koseki@iis.u-tokyo.ac.jp

Publication Details

Chiaro, G., Sato, T., Kiyota, T. & Koseki, J. (2011). Effect of initial static shear stress on the undrained cyclic behavior of saturated sand by torsional shear loading. 5th International Conference on Earthquake Geotechnical Engineering (pp. 1-12). Santiago, Chile: Chilean Geotechnical Society.

Research Online is the open access institutional repository for the University of Wollongong. For further information contact the UOW Library: research-pubs@uow.edu.au

EFFECT OF INITIAL STATIC SHEAR STRESS ON THE UNDRAINED CYCLIC BEHAVIOR OF SATURATED SAND BY TORSIONAL SHEAR LOADING

Gabriele CHIARO [1], Takeshi SATO[2], Takashi KIYOTA[3] and Junichi KOSEKI[4]

ABSTRACT

With the aim of gaining a better understanding of the role which the static shear plays on the large-deformation behavior of saturated sand, a series of undrained cyclic torsional shear tests on saturated Toyoura sand specimens up to single amplitude shear strain of about 50 % were performed. Several hollow cylinder specimens at relative density of 44 - 48 % were tested while varying the initial static shear and the subsequent cyclic shear stress levels. Depending on the degree of stress reversal, the loading pattern could be classified into three groups: stress reversal, intermediate and non-reversal. The observed failure behavior of specimens could be distinguished into liquefaction and residual deformation failures depending on the magnitude of combined static and cyclic shear stress. It was found that the presence of static shear does not always lead to an increase in the resistances to liquefaction and strain accumulation: they could either increase or decrease with increasing the static shear depending on the magnitude of combined shear stress, the type of loading and the failure behavior. As well, the mode of development of large residual deformation changed in accordance with the failure behavior which the specimen exhibited.

Keywords: large strain, liquefaction, static shear stress, torsional shear tests, undrained cyclic behavior

INTRODUCTION

Experience from past large-magnitude earthquakes (e.g., 1964 Niigata Earthquake and 1983 Nihonkai-Chubu Earthquake) indicated that extremely large horizontal ground deformation can occur in liquefied sandy deposits in coastal or river areas. When lateral spreading and flow slide take place, ground movement may exceed several meters, even in gentle slopes with an inclination of less than a few percent, resulting in severe damage to buildings, infrastructures and lifeline facilities (Hamada et al., 1994).

Soil elements within the sloped ground are subjected to an initial static shear stress on the horizontal plane or an assumed failure plane. During earthquake shaking, these elements are subjected to additional cyclic shear stress due to shear waves propagating vertically upward from the bedrock. The superimposition of static and cyclic shear stresses can have major effects on the response of soil, leading to liquefaction-induced failure of natural and artificial slopes of sandy deposits and the consequent development of extremely large ground deformation.

[1] PhD Student, Dep. of Civil Engineering, The University of Tokyo, e-mail: chiaroga@iis.u-tokyo.ac.jp
[2] Technical Director, Integrated Geotechnology Institute Ltd., tsato@iis.u-tokyo.ac.jp
[3] Associate Professor, Institute of Industrial Science, The University of Tokyo, kiyota@iis.u-tokyo.ac.jp
[4] Professor, Institute of Industrial Science, The University of Tokyo, koseki@iis.u-tokyo.ac.jp

As far as the authors have investigated in the literature, there exists no previous study on the role of initial static shear stress on the undrained cyclic behavior of saturated sand in which the strain level could exceed more than 20 %. In previous studies, in the case of simple shear tests (Vaid and Finn, 1979) or torsional shear tests (Tatsuoka et al., 1982), the shear strain level was limited to 10 % due mainly to mechanical limitation of the employed apparatus; as well, in the case of triaxial tests, due to larger extents of non-uniform deformation of the specimen at higher strain levels, the axial strain level could not exceed 20 % (Vaid and Chern, 1983; Hyodo et al., 1991, among others).

In view of the above, the purpose of this study is set to better understand the effects of initial static shear on the liquefaction behavior and to investigate the large deformation properties of saturated sand subjected to undrained torsional shear loading. In this paper, the results from investigations on the effect of initial shear stress on the undrained cyclic behavior of saturated Toyoura sand subjected to cyclic torsional shear loading up to single amplitude of shear strain of about 50 % under various combinations of static and subsequent cyclic shear stresses are presented.

TEST APPARATUS AND PROCEDURE

In this study, the torsional shear apparatus on hollow cylindrical specimens shown in Fig. 1 was employed. It is capable of achieving double amplitude torsional shear strain levels exceeding 100 % by using a belt-driven torsional loading system that is connected to an AC servo motor through electro-magnetic clutches and a series of reduction gears. To evaluate large torsional deformations, a potentiometer with a wire and a pulley was employed. The torque and axial load were detected by using a two-component load cell which is installed inside the pressure cell. The medium-size hollow cylindrical specimens employed were 150 mm in outer diameter, 90 mm in inner diameter and 300 mm in height.

All the tests were performed on Toyoura sand, which is uniform sand with negligible fines content (G_S = 2.656; e_{max} = 0.992; e_{min}= 0.632; D_{50} = 0.16; and F_C = 0.1%). Several specimens with relative density (Dr = $(e_{max} - e)/(e_{max} - e_{min})$) having a range of 44 - 48 % were prepared by air pluviation method. To minimize the degree of inherent anisotropy in radial direction of hollow cylinder sand specimens, sample preparation were carried out carefully by pouring the air-dried sand particles into a mold while moving radially the nozzle of pluviator and at the same time circumferentially in alternative directions, i.e., first in clock-wise and then anti clock-wise directions (De Silva et al., 2006). In addition, to obtain specimens with highly uniform density the falling height was kept constant throughout the pluviation process.

After being saturated, the samples were isotropically consolidated by increasing the effective stress state up to 100 kPa, with a back pressure of 200 kPa. Subsequently, the stress state was changed by applying drained monotonic torsional shear stress up a specified value. Finally, undrained cyclic torsional loading, with constant amplitude of shear stress was applied at a constant shear strain rate of 2.5 %/min. As listed in Table 1, cyclic loading tests were performed over a wide range of initial static shear varying from 0 to 20 kPa. Two levels of cyclic shear stress, 16 kPa and 20 kPa, were employed in this study in order to consider various combinations of initial static and cyclic shear stresses.

The loading direction was reversed when the amplitude of combined shear stress, which was corrected for the effect of membrane force, reached the target value. During the process of undrained cyclic torsional loading the vertical displacement of the top cap was not allowed with the aim to simulate as much as possible the simple shear condition that ground undergoes during horizontal excitation.

Table 1. Test conditions

Test	Void ratio *e*	Relative density Dr (%)	Cyclic shear stress τ_{cyclic} (kPa)	Static shear stress τ_{static} (kPa)	Combined shear $\tau_{max}=\tau_{static}+\tau_{cyclic}$(kPa) $\tau_{min}=\tau_{static}-\tau_{cyclic}$(kPa)	Type of loading
16-00	0.825	46.4	16	0	+16 / -16	Reversal
16-05	0.828	45.5	16	5	+21 / -11	Reversal
16-10	0.824	46.6	16	10	+ 26 / -6	Reversal
16-15	0.833	44.2	16	15	+ 31 / -1	Reversal
16-16	0.825	46.5	16	16	+32 / 0	Intermediate
16-17	0.820	47.9	16	17	+33 / +1	Non-Reversal
16-20	0.829	45.3	16	20	+36 / +4	Non-Reversal
20-00	0.819	48.1	20	0	+20 / -20	Reversal
20-05	0.819	48.0	20	5	+25 / -15	Reversal
20-10	0.828	45.6	20	10	+30 / -10	Reversal
20-15	0.832	44.4	20	15	+35 /-5	Reversal
20-20	0.823	46.9	20	20	+40 / 0	Intermediate

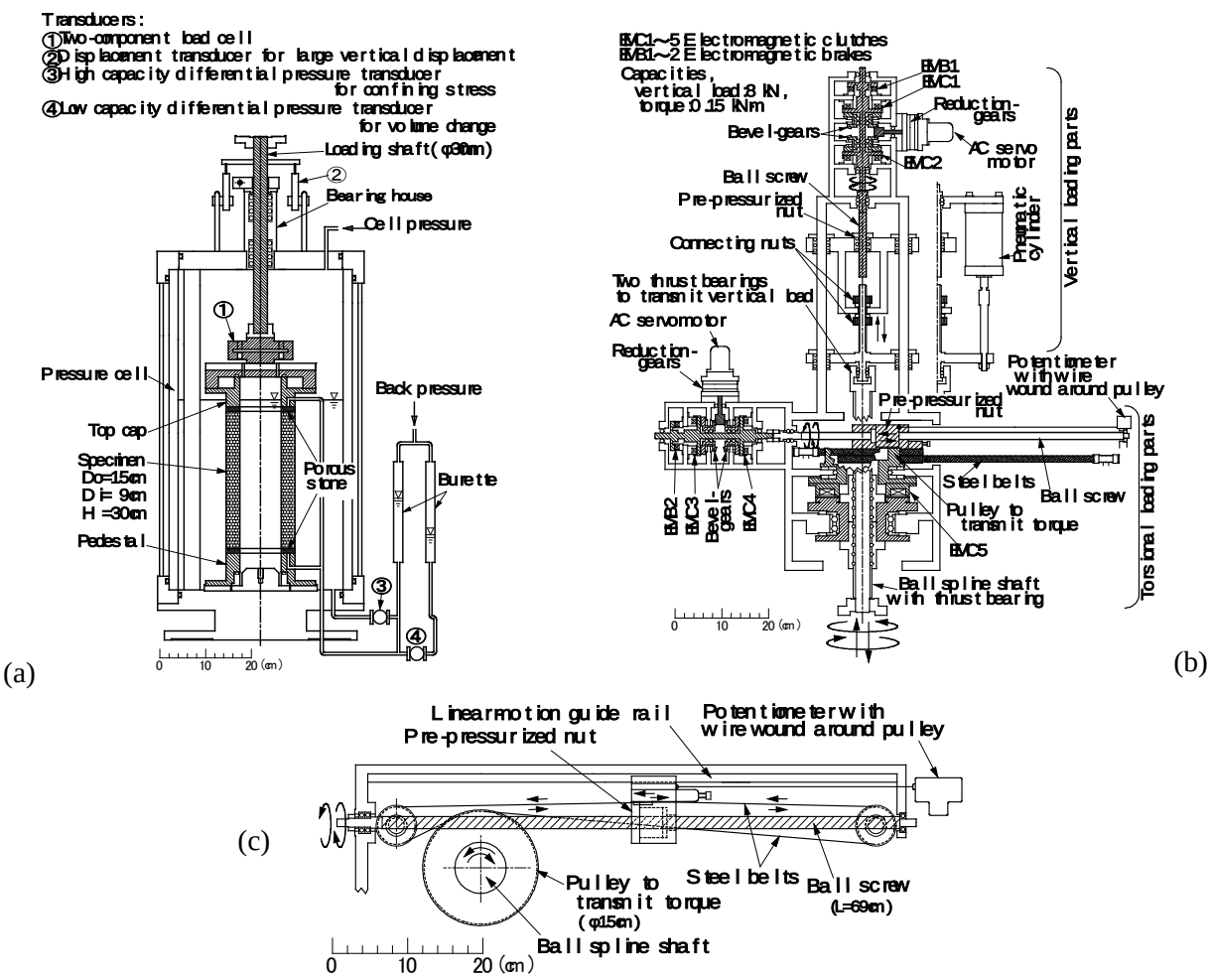

Figure1. (a) Torsional shear test apparatus on hollow cylindrical specimen; (b) Loading device; and (c) Plan view of torque-transmission part

TEST RESULTS AND DISCUSSION

Correction for membrane force

In performing torsional shear tests on hollow cylindrical specimen, due to the presence of inner and outer membranes, the effect of membrane force cannot be neglected (Koseki et al., 2007; among others). It becomes significantly important when shear strain reaches extremely high level (Kiyota et al., 2008). By employing the linear elasticity theory which uses the Young's modulus of the membrane, the theoretical apparent shear stress (τ_m) induced by the inner and outer membranes can be evaluated as follows:

$$\tau_m = \frac{t_m \, E_m \left(r_o^3 + r_i^3\right)\theta}{\left(r_o^3 - r_i^3\right)h} \tag{1}$$

Where θ is the rotational angle of the top cap detected by external potentiometer; h is the height of the specimen; r_o and r_i are the outer and inner radii of the specimen; t_m and E_m are, respectively, the thickness (=0.3mm) and the Young's modulus (=1492kPa) of membrane.

In order to confirm the validity of Eq. (1) in correcting for the effect of membrane force, a special test was performed by filling water between the inner and outer membranes and shearing the water specimen cyclically under undrained condition up to double amplitude shear strain of 100%. Fig. 2 shows both experimental and theoretical relationships between shear strain and apparent shear stress that is induced by the membranes due to torsional deformation. The deviation of the actual membrane deformation from the uniform one that is assumed in the theory became larger with increase in the strain level. Hence, in this study, the shear stress was corrected for the effect of membrane force by employing the polynomial approximation of the measured relationship between γ and τ_m as shown in Fig. 2.

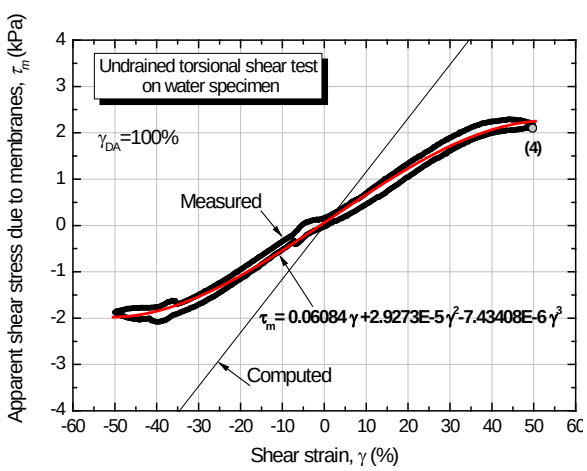

Figure 2. Relationships between τ_m due to membrane force and shear strain γ

Reversal, intermediate and non-reversal loading tests

Most of the researches that have been conducted to study the liquefaction resistance of sands are concerned with the horizontal ground in which soil elements are assumed to be subjected to fully reversed cycles of shear stress during an earthquake. However, soil elements within sloped ground are subjected to an initial static shear stress on the horizontal plane. During earthquake shaking, due to the superimposition of the static shear with the cyclic shear stress, these elements can experience partially reversed or non-reversed shear stress loading conditions.

In this study, depending on the magnitude of combined static and cyclic shear stress, the loading pattern could be classified into three groups: stress reversal, intermediate and non-reversal, as typically shown in Fig. 3. During each cycle of loading in some tests, the combined shear stress value is reversed from positive $(\tau_{max} = \tau_{static} + \tau_{cyclic} > 0)$ to negative $(\tau_{min} = \tau_{static} + \tau_{cyclic} < 0)$, or vice versa; this type of loading is called hereafter as reversal loading; whereas, the type of loading in which the reversal of loading direction is made when the value of combined shear stress (τ_{min}) achieves zero during the undrained torsional shear loading is called intermediate loading; and the one in which the combined shear stress is always kept positive is called non-reversal loading.

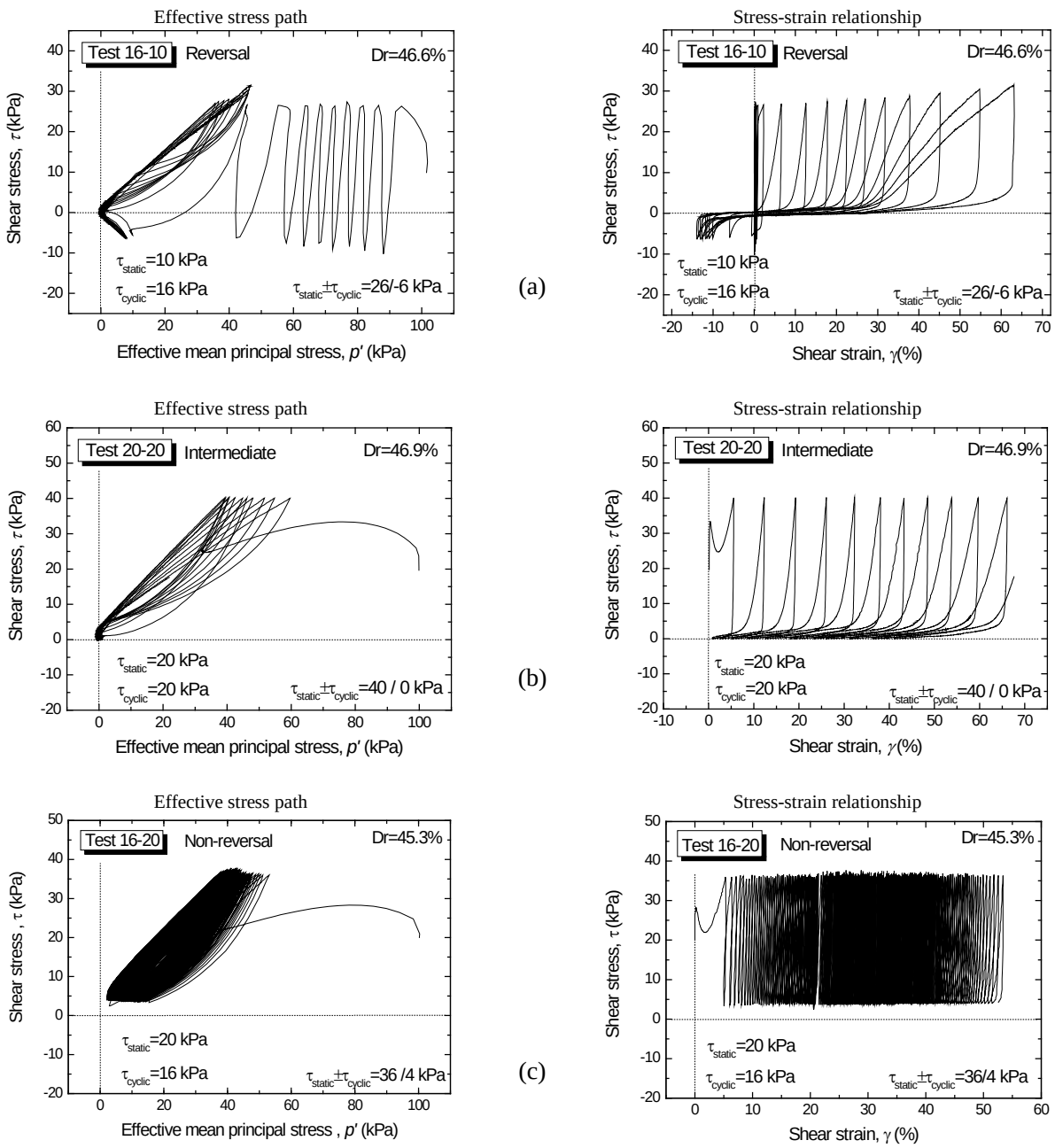

Figure 3. Typical effective stress paths and stress-strain relationships for cyclic torsional shear tests on Toyoura sand: (a) Reversal, (b) Intermediate, and (c) Non-reversal loading

Fig. 3(a) shows a typical reversal loading test result (e.g., Test 16-10) in which cyclic mobility was observed in effective stress path, where the effective stress recovered repeatedly after achieving the state of zero effective stress (i.e., full liquefaction). It was accompanied with a significant development of shear strain as evidenced by stress-strain relationship.

Fig. 3(b) illustrates a typical intermediate loading test result (e.g., Test 20-20). This type of tests shows behavior that is similar to that of reversal cases, in the sense that after reaching a fully liquefied state, progressive large deformation is developed while showing cyclic mobility.

Fig. 3(c) represents a typical non-reversal loading test result (e.g., Test 16-20). In this case, the state of zero effective stress was not achieved even after applying 208 cycles of loading; yet, even though liquefaction did not occur, a large shear strain level exceeding 50 % was reached, and formation of a single spiral shear band could be observed. The results of the above non-reversal loading test indicate that, when the combined shear stress can not achieve the zero state, full liquefaction (i.e., the zero effective stress state) does not occur.

Typical specimen deformation at large shear strain level for the case of reversal, intermediate and non-reversal tests results is shown in Photo 1. As shown in Photo 1(a), in the case of reversal tests (e.g., test 16-10) the localization of specimen deformation developed clearly in the upper part of the specimen. On the other hand, in the case of intermediate tests (e.g., test 16-16) the specimen was completely twisted, as shown in Photo 1(b). Photo 1(c) shows that in the case of non-reversal tests (e.g., test 16-20) the outer membrane was extensively wrinkled at several locations due possibly to local drainage; however, for the latter case, after the test when the zero stress state was recovered while keeping undrained condition, formation of a single spiral shear band could be observed as shown by the dotted lines in Photo 1(d). A more detailed description of these specimen deformations has been presented by Chiaro et al. (2009).

(a) γ = 63 % (b) γ = 64 % (c) γ = 50 % (d) γ = 0 % (after test)

Photo 1. Typical specimen deformation: (a) Reversal tests 16-10; (b) Intermediate test 16-16; (c) Non-reversal tests 16-20; and (d) Spiral shear band for non-reversal tests 16-20.

Effect of static shear on the failure characteristics

It is recognized from post-earthquake field investigations and many laboratory tests that soils susceptible to liquefaction consist mainly of saturated sand with uniform grain size distribution, which are deposited in loose states. However, the fact that a soil is susceptible to liquefaction does not guarantee that liquefaction will be actually initiated during an earthquake event. It is also a known fact that the stress conditions (confining pressure, cyclic shear and initial static shear stresses) play an important role in the

liquefaction behavior of soil, the type of failure mechanism and the mode of development of soil deformation, especially in the case of slopes of sandy deposits. Many studies on the liquefaction of sand, including the current one, show that under non-reversal stress conditions saturated loose sand most likely will not experience liquefaction; however, this does not mean that sand is very resistant against seismic loading; in fact, a significant magnitude of combined static and cyclic shear stresses may cause failure of soil even though liquefaction does not take place. In view of the above, it is definitely important not only to have a clear understanding of the liquefaction mechanisms, but also to carry out in depth investigation on the effects of static shear on the failure modes of saturated sandy soil during undrained shearing.

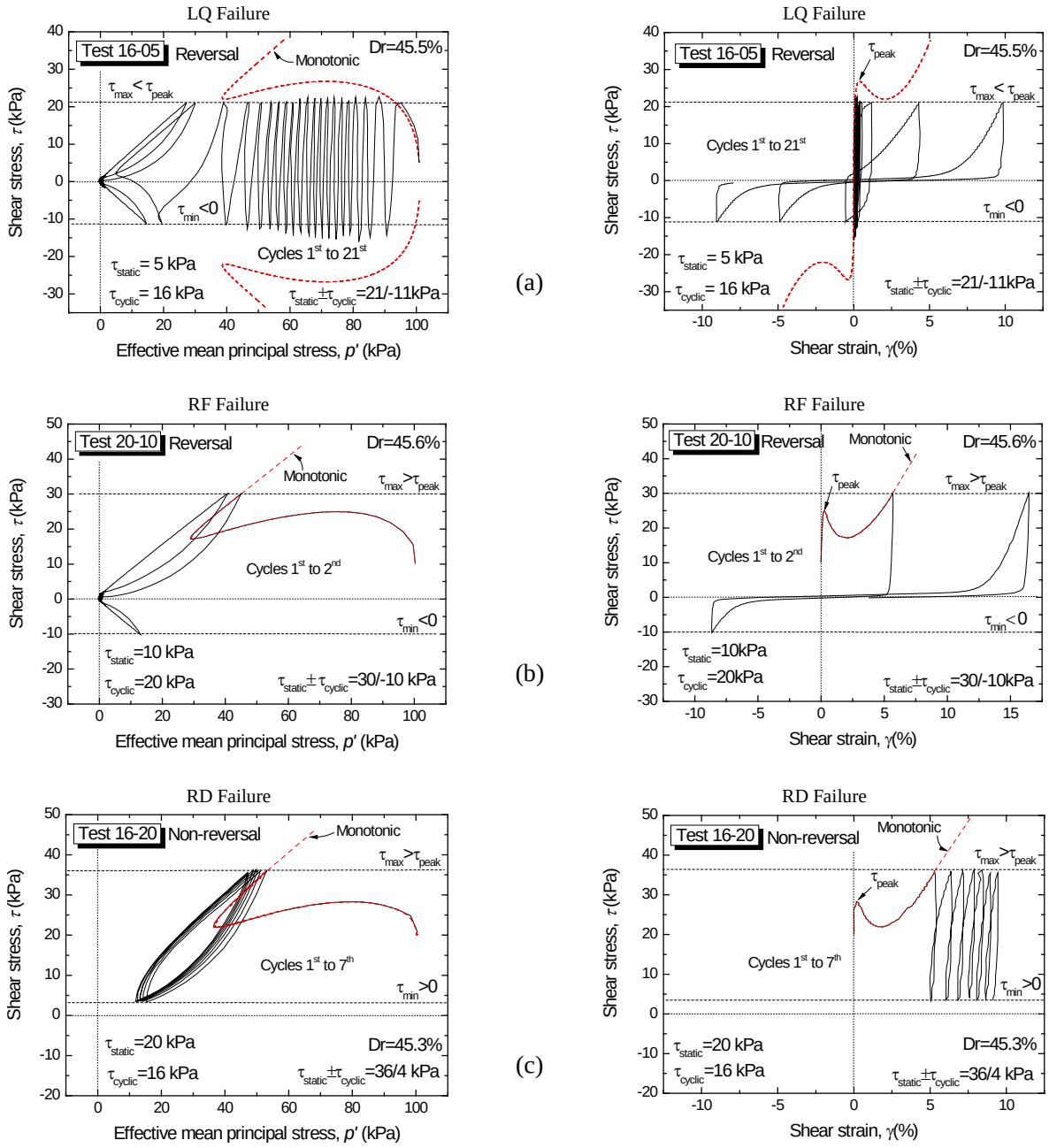

Figure 4. Observed types of failure: (a) Cyclic liquefaction failure (LQ); (b) Rapid flow liquefaction failure (RF); and (c) Residual deformation failure (RD)

In this study, the observed type of failure was distinguished into liquefaction and residual deformation based on the difference in the effective stress path and the modes of development of cyclic residual shear strain during both monotonic and cyclic loading behaviors, as shown in Fig. 4.

Cyclic liquefaction failure (LQ): In some cyclic tests, the shear stress reached a maximum value (τ_{max}) which was lower than the peak stress during undrained monotonic loading (τ_{peak}); in addition, the minimum shear stress value was negative ($\tau_{min}<0$). Under these stress conditions (i.e., reversal stress), while undergoing several tens of cycles, due to the excess pore water pressure generation, the effective mean principal stress (p') progressively decreased and the stress state moved toward the failure envelope and finally reached the full liquefaction state ($p'=0$). Then, in the post liquefaction process, large deformations were developed. Fig 4(a) shows a typical test result of cyclic liquefaction failure (LQ).

Rapid flow liquefaction failure (RF): In other tests, the shear stress reached a maximum value which was higher than the peak stress during undrained monotonic loading ($\tau_{max} > \tau_{peak}$), while due to stress reversal or intermediate conditions the minimum shear stress value was negative ($\tau_{min}<0$) or zero ($\tau_{min}=0$), respectively. As a result, liquefaction took place mostly in-between the first cycle of loading (few cycles for intermediate tests) and a rapid development of residual strain was observed. A typical test result of rapid flow liquefaction failure (RF) is shown in Fig. 4 (b).

Residual deformation failure (RD): In some tests the shear stress reached a maximum value which was higher than the peak stress during undrained monotonic loading ($\tau_{max} > \tau_{peak}$), as well as the minimum shear stress value was positive ($\tau_{min}>0$). Under these stress conditions (i.e., non-reversal stress), during cyclic loading large deformations were achieved, while liquefaction was not reached even after applying a hundred of cycles. As a result, residual deformation brought the sample to failure. Fig. 4(c) illustrates a typical test result of residual deformation failure (RD).

Resistance to liquefaction and cyclic strain accumulation

Usually, the resistance to liquefaction or cyclic strain accumulation is expressed by the cyclic stress ratio ($CRS = \tau_{cyclic} / p'_0$) required to develop a specific amount of deformation from the initial configuration of the specimen or during cyclic loading (i.e., single or double amplitude shear strain). However, in many cases, it can be seen that cyclic stress ratio is not a sufficient single parameter to describe the effects of initial static shear on the resistance to liquefaction or cyclic strain accumulation. Therefore, in this study, to address this issue, the liquefaction resistance curves were described in terms of both the cyclic stress ratio ($CSR= \tau_{cyclic} / p'_0$) and the static stress ratio ($SSR= \tau_{static} / p'_0$), as listed in Table 2.

Table 2. Liquefaction, strain accumulation and failure characteristics

Test	$SSR=\tau_{static}/p_0'$	$CSR=\tau_{cyclic}/p_0'$	N_{20} (γ_{SA}=20%)	N_{50} (γ_{SA} =50%)	Type of failure
16-00	0.00	0.16	38	48	LQ
16-05	0.05	0.16	26	33	LQ
16-10	0.10	0.16	13	20	LQ
16-15	0.15	0.16	3.2	6.9	RF
16-16	0.16	0.16	4.0	13	RF
16-17	0.17	0.16	13	30	RD
16-20	0.20	0.16	46	202	RD
20-00	0.00	0.20	6.3	18	LQ
20-05	0.05	0.20	4.4	14	LQ
20-10	0.10	0.20	2.0	6.9	RF
20-15	0.15	0.20	2.0	5.7	RF
20-20	0.20	0.20	2.6	7.8	RF
p_0'= initial effective mean principal stress (=100 kPa) LQ: cyclic liquefaction failure; RF: rapid flow liquefaction failure; RD: residual deformation failure					

To describe the resistance to liquefaction, double amplitude shear strain (γ_{DA}) and/or single amplitude shear strain at the maximum shear stress state ($\gamma_{SA,\tau=\tau max}$) are typically used. However, as schematically shown in Fig. 5, in using initial static shear, the stress conditions become non-symmetric with respect to the initial stress state; as a result γ_{DA} is not well representative of the strain accumulation during cyclic loading. Therefore, in the current study, to be consistent with previous relevant studies (Tatsuoka et al., 1982; among others), the resistance to liquefaction (or more strictly, resistance to cyclic strain accumulation) was evaluated in terms of number of cycles required to develop a specific amount of single amplitude shear strain (γ_{SA}). Effect of membrane penetration due to pore water pressure generation on liquefaction resistance (e.g., Koseki et al., 2005; among others) was not considered in this study since it results independent from the level of initial static shear applied.

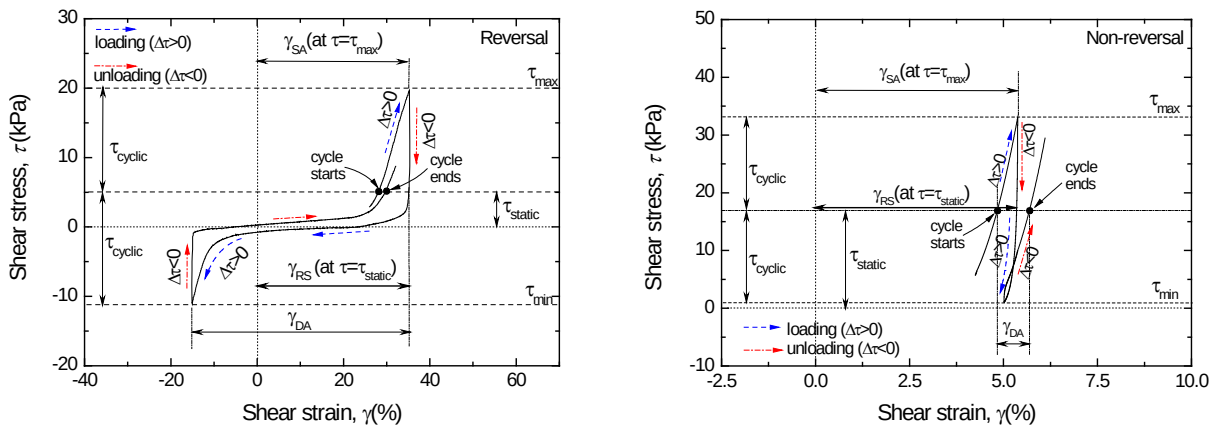

(a) (b)

Figure 5. Definition of shear strain components: (a) Stress reversal and (b) Non-reversal loading conditions

Fig. 6 and Fig. 7 show that, the number of cycles to achieve γ_{SA}= 20 % and γ_{SA} = 50 %, first decreases and then increases with increasing the static shear stress. This two-phase change in strain accumulation behavior can be associated with a two-phase change in failure behavior, from LQ to RF and from RF to RD. It may be noted also that, for a given value of static shear, the resistance to liquefaction decreases with increasing the amplitude of cyclic stress; this response is in accordance with those observed in previous studies, such as Vaid and Finn (1979), Vaid and Chern (1983), Hyodo et al. (1991), among others. It should be also noted that, by the current study for the first time the effects of initial static shear on the resistance against cyclic shear strain accumulation of γ_{SA} = 50 % could be investigated and described, as shown in Fig. 6(b) and Fig. 7(b).

In conclusion, these tests results show that the presence of initial static shear does not always lead to an increase in the resistances against liquefaction and strain accumulation. They can either increase or decrease depending on the magnitude of the combined shear stress and the type of loading (i.e., degree of reversal stress), and the failure behaviors.

Mode of residual deformation development

In accordance with Tatsuoka et al. (1982), the value of γ_{SA} may be used to estimate values of cyclic shear strain amplitude during earthquakes; on the other hand, the residual deformation of slopes just after earthquakes can be estimated by defining the shear strain level at zero cyclic shear stress. Therefore, in the current study, to examine the effects of initial static shear on the deformation properties of saturated loose sand in undrained cyclic torsional shear tests, the residual shear deformation (γ_{RS}), measured in

terms of single amplitude shear strain at the moment when the stress state recovered the initial value of static shear stress (i.e., zero cyclic shear stress applied) during the unloading stage of each cycle (i.e., at $\tau = \tau_{static}$, $d\tau < 0$), as defined in Fig. 5, was employed. It should be noted that, in the tests presented in this paper, γ_{RS} and γ_{SA} differ at maximum of about 1 – 2 %.

Based on the failure behavior of each specimen, three types of mechanisms of residual strain development could be identified, as shown in Fig. 8.
Fig 8(a) summarizes the residual deformation behavior of specimens showing cyclic liquefaction failure behavior (LQ). In these tests, full liquefaction state ($p'=0$) was achieved after applying several cycles of loading; then, a sudden development of residual shear deformation took place.
Fig. 8(b) illustrates the behavior of specimens characterized by rapid flow liquefaction failure mode (RF). In this case, during the first cycle, full liquefaction and shear deformation of a few percent were achieved. In addition, in most of the tests, deformation exceeding 50% was reached in less than 10 cycles.
Fig. 8(c) shows the case of residual deformation failure (RD). These tests show that, extremely large deformation could be reached after applying a large number of cycles of loading, even in the case in which liquefaction did not take place.

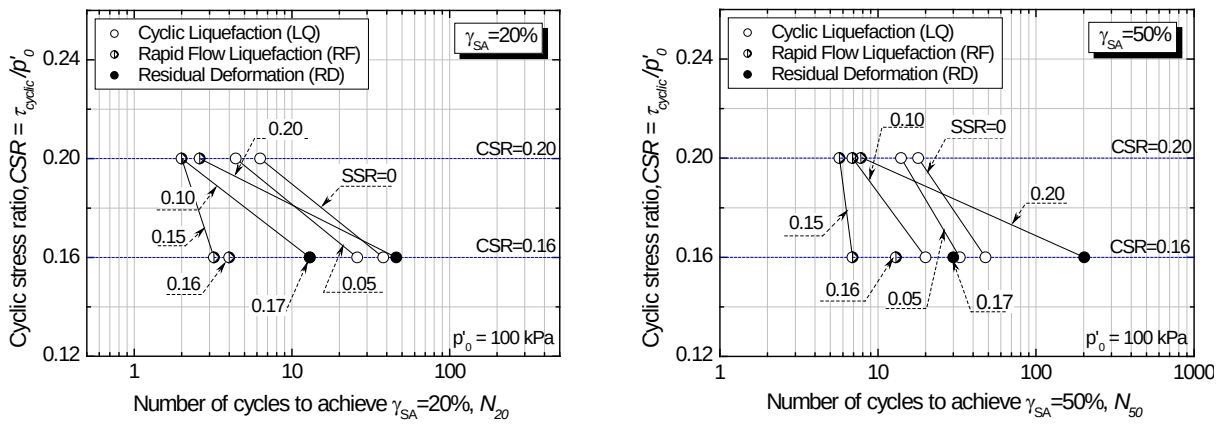

(a) (b)

Figure 6. Relationship between cyclic stress ratio and number of cycles to cause: (a) Single amplitude shear strain of 20%; (b) Single amplitude shear strain of 50%

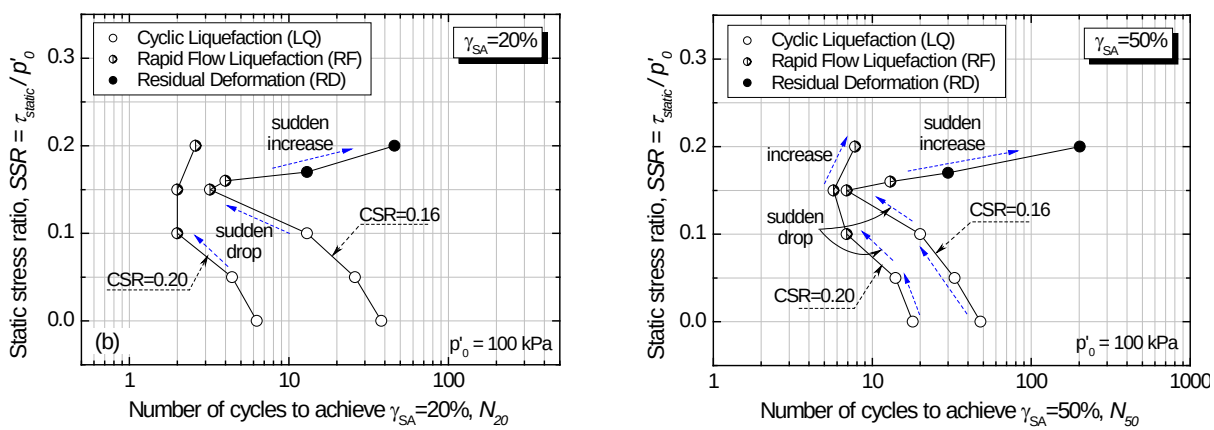

(a) (b)

Figure 7. Relationship between static stress ratio and number of cycles to cause: (a) Single amplitude shear strain of 20%; (b) Single amplitude shear strain of 50%

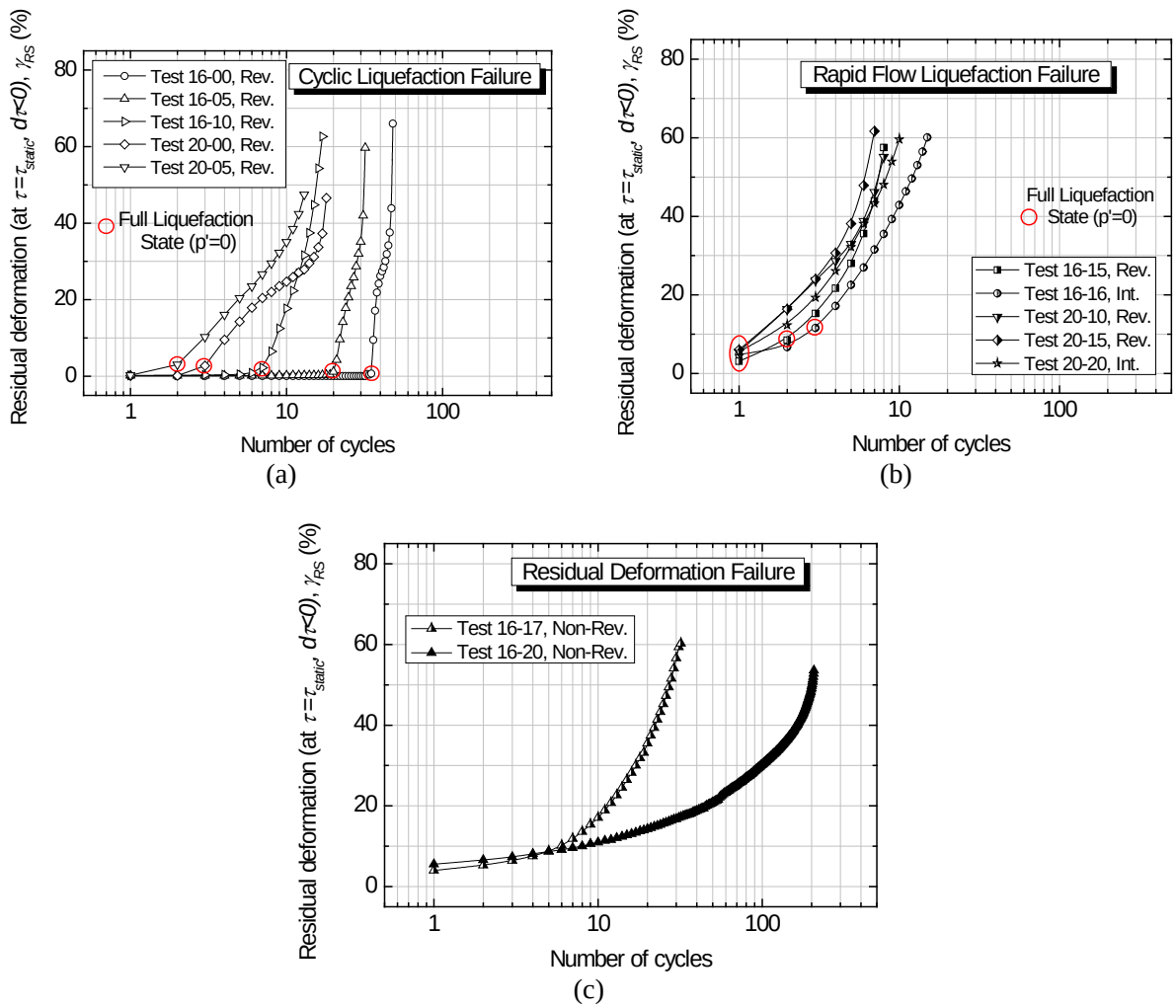

Figure 8. Modes of development of residual deformation during undrained cyclic torsional loading: (a) Results of LQ failure behavior tests; (b) Results of RF failure behavior tests; and (c) Results of RD failure behavior tests

CONCLUSIONS

In order to investigate the effects of initial shear stress on the large deformation properties of loose sand, a series of undrained cyclic torsional shear tests were performed on loose saturated Toyoura sand specimens up to single amplitude of shear strain of about 50 % under various combinations of static and subsequent cyclic shear stresses. The following conclusions can be drawn from the above study:

(i) Depending on the relative magnitude of initial static shear and the cyclic shear stresses, the cyclic loading paths could be classified into three groups: stress reversal, intermediate and non-reversal.

(ii) From the study of failure mechanisms, based on the difference in the effective stress path and the modes of development of shear strain of both monotonic and cyclic behaviors, the observed types of failure could be distinguished into three types: cyclic liquefaction (LQ), rapid flow liquefaction (RF) and residual deformation (RD) failures. In case of stress reversal and intermediate loadings, failure was

associated with full liquefaction, followed by extremely large deformation in the post-liquefaction process. On the other hand, in the case of non-reversal loading, it was found that residual deformation brought the specimen to failure (i.e., formation of spiral shear band) although liquefaction did not occur.

(iii) The test results show that the presence of initial static shear does not always lead to an increase in the resistance to liquefaction and shear strain accumulation up to 50%; in fact, both can either increase or decrease by increasing the static shear depending on the magnitude of the combined shear stress, the type of loading and the failure behavior.

(iv) The mechanisms of residual strain development clearly depend on the failure behavior of sands. In the case of LQ failure, full liquefaction state ($p'=0$) was achieved after applying several cycles of loading followed by a sudden development of residual deformation. On the other hand, in the case of RF failure, during the first cycle, full liquefaction and deformation of a few percent was achieved; in addition, in most of the tests, a residual shear exceeding 50% was reached in less than 10 cycles. On the contrary, in the case of RD failure, extremely large deformation could be reached after applying a large number of cycles of loading, although liquefaction did not take place.

REFERENCES

Chiaro, G., Kiyota, T., De Silva, L. I. N., Sato, T. and Koseki, J. (2009): Extremely large post-liquefaction deformations of saturated sand under cyclic torsional shear loading. Proc. of TC4, Earthquake Geotechnical Engineering Satellite Conference, 17th ICSMGE, Alexandria, Egypt, CD-ROM, Paper-ID: 03.

De Silva, L.I.N., Koseki, J., and Sato, T. (2006). Effects of different pluviation techniques on deformation property of hollow cylinder sand specimens. Proc. of the International Summer Symposium on Geomechanics and Geotechnics of Particulate Media, Ube, Yamaguchi, Japan, pp. 29-33.

Hamada, M., O'Rourke, T.D. and Yoshida, N. (1994). Liquefaction-induced large ground displacement. Performance of Ground and Soil Structures during Earthquakes, 13th ICSMFE, JGS, pp. 93-108.

Hyodo, M., Murata, H., Yasufuku, N., and Fujii, T. (1991). Undrained cyclic shear strength and residual shear strain of saturated sand by cyclic triaxial tests. Soils and Foundations, Vol. 31, No. 3, pp. 60-76.

Kiyota, T., Sato, T., Koseki, J., and Mohammad, A. (2008). Behavior of liquefied sands under extremely large strain levels in cyclic torsional shear tests. Soils and Foundations, Vol. 48, No. 5, pp. 727-739.

Koseki, J., Kiyota, T., Sato, T. and Mohammad, A.M. (2007). Undrained cyclic torsional shear tests on sand up to extremely large strain levels. International Workshop on Earthquake Hazard and Mitigation, Guwahati, India, pp. 257-263.

Koseki, J., Yoshida, T. and Sato, T. (2005): Liquefaction properties of Toyoura sand in cyclic torsional shear tests under low confining stress. Soils and Foundations, Vol. 45, No. 5, pp. 103-113.

Tatsuoka, F., Muramatsu, M. and Sasaki, T. (1982). Cyclic undrained stress-strain behavior of dense sand by torsional simple shear test. Soils and Foundations, Vol. 22, No. 2, pp. 55-69.

Vaid, Y.P. and Chern, J.C. (1983). Effects of static shear on resistance to liquefaction. Soils and Foundations, Vol. 23, No. 1, pp. 47-60.

Vaid, Y.P. and Finn, W.D.L. (1979). Static shear and liquefaction potential. Journal of the Geotechnical Engineering Division, Proc. ASCE, Vol. 105, No. GT10, pp. 1233-1246.